Available online at www.sciencedirect.com

SciVerse ScienceDirect

Ceramics International 39 (2013) 2949–2954

CERAMICS INTERNATIONAL

www.elsevier.com/locate/ceramint

Temperature-independent and enhanced dielectric properties for two-layer structure capacitors with $0.8Pb(Fe_{2/3}W_{1/3})O_3$–$0.2PbTiO_3$–MnO and $0.7Pb(Fe_{2/3}W_{1/3})O_3$–$0.3PbTiO_3$–MnO ceramics

Cheng-Shong Hong[a,*], Sheng-Yuan Chu[b,c,**], Cheng-Che Tsai[d], Wen-Chang Su[b], Hsiu-Hsien Su[b]

[a]*Department of Electronic Engineering, National Kaohsiung Normal University, Kaohsiung 824, Taiwan, ROC*
[b]*Department of Electrical Engineering, National Cheng Kung University, Tainan 701, Taiwan, ROC*
[c]*Center for Micro/Nano Science and Technology, National Cheng Kung University, Tainan 701, Taiwan, ROC*
[d]*Department of Electronics Engineering and Computer Science, Tung Fang Design University, Kaohsiung County 829, Taiwan, ROC*

Received 3 June 2012; received in revised form 22 September 2012; accepted 22 September 2012
Available online 28 September 2012

Abstract

This study fabricates capacitors with two-layer structure and different compositions, $0.8Pb(Fe_{2/3}W_{1/3})O_3$–$0.2PbTiO_3$–MnO and $0.7Pb(Fe_{2/3}W_{1/3})O_3$–$0.3PbTiO_3$–MnO, by using the conventional solid state oxide reaction method. By using the temperature compensation effect and adjusting the thickness ratio of the two layers with different compositions, the temperature–dielectric peak is enhanced and smoothed. The dielectric loss, space charge polarization and dc conduction are suppressed at the highest temperature region. Furthermore, the Maxwell–Wagner model is used to fit and explain the dielectric behaviors. This study also provides suggestions and discussion related to the effect of the interfacial region based on the experimental data and fitting results.

Keywords: Temperature Compensation; Maxwell–Wagner; Dielectric; Relaxor

1. Introduction

A typical relaxor ferroelectric (RFE) usually exhibits a perovskite structure $A(B_1B_2)O_3$, a high dielectric constant, a broad temperature–dielectric peak and frequency dispersion [1–5]. To obtain a higher dielectric constant and broader temperature–dielectric peak, the binary and trinary systems are usually synthesized with multiple compositions or by doping some additives [6–14]. Although a broader temperature–dielectric peak can be enhanced by multiple compositions, however temperature-independent dielectric peaks cannot yet be realized because the diffused phase transitions corresponding to the maximum values of the temperature–dielectric constant are still existent for RFE materials.

Recently, the Maxwell–Wagner model has typically been used to investigate the dielectric relaxation of multi-layer structure with different composition mediums, such as the surface-layer effect of internal barrier layer capacitors [15–23], the superlattice effect of ferroelectric thin film depositions [23–26], and the giant and temperature independence of multiferroic and magnetoelectric materials [23,27–29]. Furthermore, the microwave dielectric properties are also modified by the layered structure for bulk devices [30,31]. According to the above reports, the temperature-independent dielectric constant can be realized by using the Maxwell–Wagner effect for the two-layer capacitors with different compositions. However, to date,

*Corresponding author. Tel.: +886 7 7172930 x7915; fax: +886 7 6051330.
**Corresponding author at: Department of Electrical Engineering, National Cheng Kung University, Tainan 70101, Taiwan, ROC. Tel.: +886 6 2757575 x62381; fax: +886 6 2345482.
E-mail addresses: cshong@nknu.edu.tw (C.-S. Hong), chusy@mail.ncku.edu.tw (S.-Y. Chu).

0272-8842/$ - see front matter © 2012 Elsevier Ltd and Techna Group S.r.l. All rights reserved.
http://dx.doi.org/10.1016/j.ceramint.2012.09.070

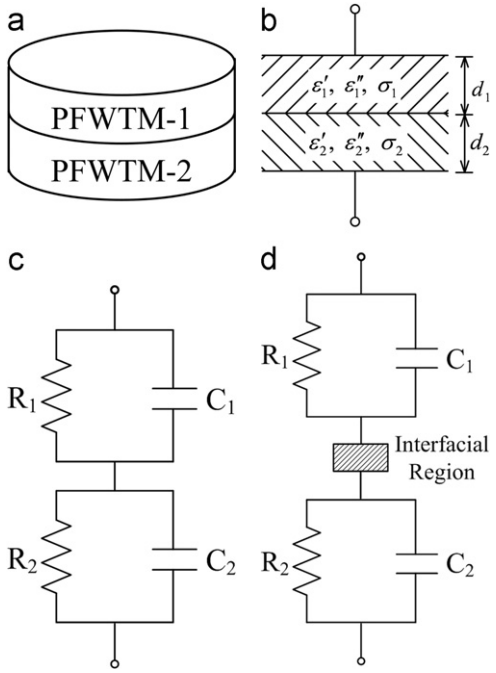

Fig. 1. (a) Configuration, (b) schematic structure of Maxwell–Wagner model, (c) equivalent circuit and (d) equivalent circuit with interfacial region for the two-layers structure capacitors with different compositions.

few studies have discussed the relaxor characteristics of the layered structure for bulk devices.

$xPb(Fe_{2/3}W_{1/3})O_3$–$(1-x)PbTiO_3$ ($xPFW-(1-x)PT$) is a typical binary RFE material. The temperatures T_m corresponding to the maximum value of the temperature–dielectric constant, the dielectric properties and the lattice structures can be changed by controlling the $PbTiO_3$ contents [6–9]. Furthermore, the broad temperature–dielectric peak is enhanced and the dielectric loss is suppressed by doping MnO additives [10]. In addition, 0.8PFW-0.2PT-0.15 wt% MnO (PFWTM-1) and 0.7PFW-0.3PT-0.15 wt% MnO (PFWTM-2) can be fine sintered at 880 °C and their temperatures corresponding to the maximum value of the temperature–dielectric constant are −16 °C and 33 °C, respectively, at 1 MHz [10]. In the present work, the different compositions, PFWTM-1 and PFWTM-2, are compacted into the disk of a two-layer structure, as shown in Fig. 1(a), with different thickness ratios. This study investigates the effects of the thickness ratio and the temperature compensation on the low field dielectric response. Moreover, we also discuss the Maxwell–Wagner effects and provide suggestions in regard to the interfacial region.

2. Experiment and ceramic preparation

Raw materials were mixed and milled using pure reagent PbO, Fe_2O_3, WO_3, TiO_2 and MnO powders (99.5% purity). The materials $0.8Pb(Fe_{2/3}W_{1/3})O_3$–$0.2PbTiO_3$-0.15 wt% MnO and $0.7Pb(Fe_{2/3}W_{1/3})O_3$–$0.3PbTiO_3$-0.15 wt% MnO were synthesized by calcining at 750 °C for 2 h. The calcined powders were remilled in alcohol and dried again. After that, the fine calcined powders were obtained and some different preparative routes were followed as described below:

(1) single-layer structure: $0.8Pb(Fe_{2/3}W_{1/3})O_3$–$0.2PbTiO_3$-0.15 wt% MnO calcined powders were pressed into pellets of 12 mm in diameter and 0.5 mm thickness (called PFWTM-1). $0.7Pb(Fe_{2/3}W_{1/3})O_3$–$0.3PbTiO_3$-0.15 wt% MnO calcined powders were pressed into pellets of 12 mm in diameter and 0.5 mm thickness (called PFWTM-2).
(2) two-layer structure: $0.8Pb(Fe_{2/3}W_{1/3})O_3$–$0.2PbTiO_3$-0.15 wt% MnO (PFWTM-1) and $0.7Pb(Fe_{2/3}W_{1/3})O_3$–$0.3PbTiO_3$-0.15 wt% MnO (PFWTM-2) calcined powders were compactly pressed into pellets of 12 mm in diameter with two-layer structure and different thickness ratios as shown in Fig. 1(a) (called 1:1 PFWTM, 2:1 PFWTM and 3:1 PFWTM of which the thickness ratios of PFWTM-1 and PFWTM-2 were 1:1, 2:1 and 3:1.). The thicknesses of PFWTM-1 and PFWTM-2 are 0.5 mm and 0.5 mm for 1:1 PFWTM, 1 mm and 0.5 mm for 2:1 PFWTM and 1.5 mm and 0.5 mm for 3:1 PFWTM, respectively.

These pressed pellets were sintered at the same sintering temperature of 880 °C for 2 h. In order to measure the dielectric properties, silver paste was coated to form electrodes on both sides of the sintered samples, and then subsequently fired at 750 °C for 25 min. The dielectric properties of the samples were measured using an impedance analyzer (HP4294A) in a temperature-controllable furnace. The phase relations for the sintered samples were identified using an x-ray diffractometer with Siemens D5000, operated at 40 kV/40 mA and room temperature with Cu Kα radiation (λ=0.154 nm). The microstructures were observed using a scanning electron microscope SEM (Hitachi S-3000 N microscope). The X-ray patterns and the SEM images of the PFWTM-1 and PFWTM-2 ceramics had been discussed in the previous study and shown pure perovskite structures and no pyrochlore phase [32]. Furthermore, both sides of the 1:1 PFWTM, 2:1 PFWTM and 3:1 PFWTM samples show similar X-ray patterns and SEM images. Since the PFWTM-1 and PFWTM-2 samples have different compositions and different shrinkages (10.65% and 10.81% for PFWTM-1 and PFWTM-2 separately), it is reasonably suggested that the interfacial regions and cracks are existent for the layered structure capacitor [30,31]. However, the boundary of the PFWTM-1 and PFWTM-2 ceramics for the 1:1 PFWTM, 2:1 PFWTM and 3:1 PFWTM samples could not be found by using XRD diffractometer since it is too thin and cannot be identified from both sides of the two-layer samples. Fig. 2 (a) and (b) show the profiled SEM images with different magnifications for the two-layer capacitors, 2:1 PFWTM. In Fig. 2, the boundaries and

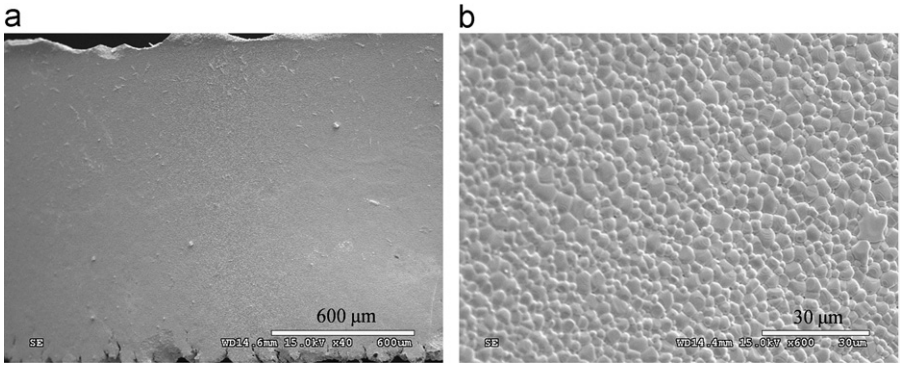

Fig. 2. The profiled SEM images with different magnifications (a) ×40 multiples (b) ×600 multiples for 2:1 PFWTM ceramics.

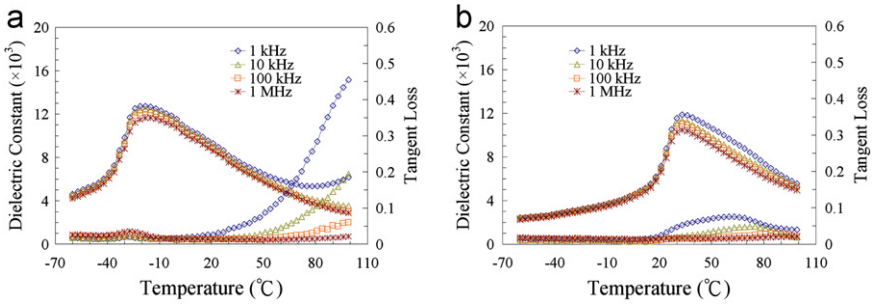

Fig. 3. Dielectric constant and tangent loss as a function of temperature at different frequencies for (a) PFWTM-1 and (b) PFWTM-2 ceramics with single-layer structure [10].

cracks cannot be founded. These results are different with the previous reports [30,31]. It is suggested that the compositions and shrinkages are closed between PFWTM-1 and PFWTM-2. However the boundaries and cracks cannot be identified, we still believe that the interfacial regions exist at the boundary.

3. Results and discussion

Fig. 3 shows the dielectric constant and the tangent loss as a function of temperature at different frequencies for (a) PFWTM-1 and (b) PFWTM-2 ceramics with single-layer structure. In Fig. 3 (a) and (b), the temperature T_m corresponding to the maximum temperature–dielectric constant is increased and the temperature–dielectric peak is sharpened by increasing $PbTiO_3$ contents since $PbTiO_3$ has a high Curie temperature of 490 °C and a typical ferroelectric property with a sharp phase transition [9,10]. Therefore, it is concluded that the characteristic of phase transition is changed from a diffused SRO (short range order) relaxor state to a sharp LRO (long range order) ferroelectric state by increasing $PbTiO_3$ contents. The details have been discussed in the previous studies [9,10]. In the paraelectric region of Fig. 3(a), the dielectric constant is increased again and the tangent loss is obviously enhanced by increasing the measured temperature at the highest temperature region (> 50 °C). Zhou et al. suggested that the response mechanism is relative to the space charge polarization and the electron hole [4,5]. When the frequency is increased, the phenomenon vanishes since the relaxation time of these polarizations is too long to follow the external field.

Fig. 4 shows the dielectric constant and the tangent loss as a function of temperature for (a) 1:1 PFWTM, (b) 2:1 PFWTM and (c) 31:1 PFWTM ceramics with two-layer structure capacitors at different frequencies. Inspecting the experimental data of Fig. 4 (a), (b) and (c), two temperature–dielectric peaks are shown with the dashed line. There are consistent with the diffused phase transition temperatures corresponding to the maximum dielectric constant of the PFWTM-1 and PFWTM-2 ceramics. Furthermore, the temperature–dielectric constant between two dashed line (the temperature compensation range), as shown in Fig. 4, are smoothed because the temperature compensation effect of the PFWTM-1 and PFWTM-2 ceramics. In this temperature range, the temperature–dielectric constants are decreased for one layer of the PFWTM-1 ceramics, and are increased for another layer of the PFWTM-2 ceramics when the measured temperatures are increased. In particular, the temperature-independent dielectric peak is obtained at a temperature range of –20 °C–28 °C for the 2:1 PFWTM two-layer structure, as shown in Fig. 4(b). Since the two-layer structure capacitors shown in Fig. 4 are compacted with the PFWTM-1 and PFWTM-2 ceramics, the dielectric properties of the two-layer structure should exhibit the dielectric properties of the PFWTM-1 and PFWTM-2 ceramics at

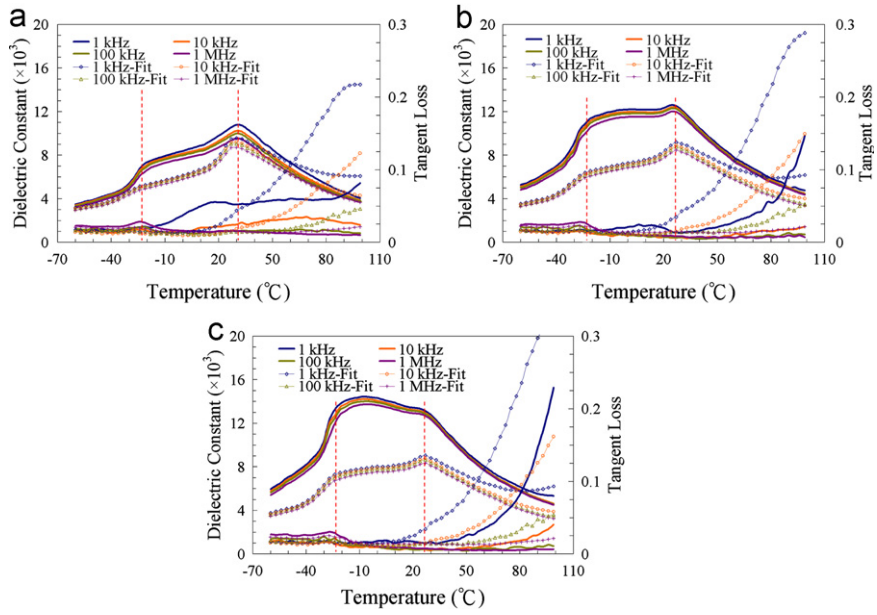

Fig. 4. The experimental data and the fitting results of the dielectric constant and the tangent loss as a function of temperature at different frequencies for (a) 1:1 PFWTM, (b) 2:1 PFWTM and (c) 3:1 PFWTM ceramics with two-layer structure.

the same time. Moreover, the dielectric properties of the PFWTM-1 ceramics should be enhanced for the two-layer structure capacitor when the thickness of PFWTM-1 ceramics is increased. In Fig. 3 (a) and (b), the temperature corresponding to the maximum temperature–dielectric constant of the PFWTM-1 ceramics is lower than that of the PFWTM-2 ceramics, and the dielectric loss of the PFWTM-1 ceramics is higher than that of the PFWTM-2 ceramics at the highest temperature ranges ($>50\,^{\circ}C$). Therefore, for the two-layer structure capacitors the temperature–dielectric constant near the lower temperature–dielectric peak is enhanced and the dielectric loss at the higher temperature is increased when the thickness of PFWTM-1 ceramics is increased, as shown in Fig. 4. In addition, it is unexpectedly found that the dielectric constants are not only compensated but also enhanced in the temperature compensation range (between two dashed lines shown in Fig. 4 (a), (b) and (c).). The enhanced effects are more obvious when the thicknesses of the PFWTM-1 ceramics are increased. These peculiar and interesting results are systematically discussed as below.

To further clarify the effect of the thickness for the two-layer structure capacitors with different compositions on the dielectric properties, the experimental data of Fig. 3 (a) and (b) are used to fit by using the Maxwell–Wagner model with different thickness ratios according to the structure and equivalent circuit of the two-layer structure capacitors shown in Fig. 1 (b) and (c). These equations are shown as [21–28]:

$$\varepsilon^*(\omega) = \varepsilon_\infty + \frac{\varepsilon_s - \varepsilon_\infty}{1 + j\omega\tau} - j\frac{\varepsilon_0}{\omega\tau_0} \tag{1}$$

$$\varepsilon_\infty = \frac{d\varepsilon_1'\varepsilon_2'}{\varepsilon_1' d_2 + \varepsilon_2' d_1} \tag{2}$$

$$\varepsilon_s = d\frac{d_1\varepsilon_1'\sigma_2^2 + d_2\varepsilon_2'\sigma_1^2}{(d_2\sigma + d_1\sigma_2)^2} \tag{3}$$

$$\tau = \frac{d_2\varepsilon_1' + d_1\varepsilon_2'}{d_2\sigma_1 + d_1\sigma_2} \tag{4}$$

$$\tau_0 = \frac{\varepsilon_0}{d} \times \frac{d_2\sigma_1 + d_1\sigma_2}{\sigma_1\sigma_2} \tag{5}$$

$$\sigma_1 = \omega\varepsilon_1'', \quad \sigma_2 = \omega\varepsilon_2'', \; d = d_1 + d_2 \tag{6}$$

where ε_1' and ε_1'' (ε_2' and ε_2'') are the real and imaginary parts of the complex relative permittivity of PFWTM-1 (PFWTM-2) ceramics. d_1 and d_2 are the thicknesses of PFWTM-1 and PFWTM-2 ceramics. ω and ε_o are the angular frequency and the relative permittivity of free space. The fitting results of the Maxwell–Wagner effect are shown in Fig. 4 (a), (b) and (c) together with the experimental data. Comparing the fitting results and the experimental data, the temperature–dielectric constant is smoothed in the temperature compensation range (between two dashed lines shown in Fig. 4) and is sharpened at the lowest and highest temperature range according to the thickness ratios of PFWTM-1 and PFWTM-2 ceramics. The phenomena are consistent between the experimental data and the fitting results shown in Fig. 4 (a), (b) and (c). Furthermore, the dielectric constant (experimental data) is enhanced at all temperature ranges for all two-layer structure capacitors. In particular, the enhanced effect of the dielectric constant is more strengthened at the temperature compensation range by increasing the PFWTM-1 thickness. The enhancements of the temperature–dielectric constant are inconsistent with the fitting results using the Maxwell–Wagner model shown in Fig. 4 (a), (b) and (c). Since the two-layer structure capacitors are compacted with different

composition and then sintered, it is inferred that the interfacial regions should exist at the boundary between the PFWTM-1 and PFWTM-2 ceramics. Furthermore, the thicknesses and compositions of the interfacial region should be the same between the two-layer structure capacitors of the 1:1 PFWTM, 2:1 PFWTM and 3:1 PFWTM since these samples are compacted with the same calcined powders, PFWTM-1 and PFWTM-2, and sintered at the same temperature (880 °C) for the same time (2 h). Therefore, the enhanced effect of the dielectric constant can be attributed to the interfacial region [23–26] and the equivalent circuit is shown in Fig. 1(d). According to the previous reports [23–26], the interfacial region has low resistivity and its resistivity is decreased by increasing the temperature, in obeisance of the Arrhenius law. Although the interfacial region can be used to explain the enhanced effect of the dielectric constant, it cannot explain why the enhanced degree is strengthened by increasing the PFWTM-1 thickness, since the thicknesses and compositions of the interfacial region should be the same for the two-layer structure capacitors of the 1:1 PFWTM, 2:1 PFWTM and 3:1 PFWTM.

As mentioned above, the Maxwell–Wagner model with the low resistivity interfacial region can explain the temperature-independent dielectric peak and the enhancement of the dielectric constant. In addition, this model always accompanies a high dielectric loss because of the low resistivity interfacial region [23–26]. Comparing the experimental data and the fitting results of the temperature-tangent loss in Fig. 4, there is no obvious difference at a low temperature range (< -16 °C) and the experimental data is slightly enhanced only at a low frequency and at the temperature compensation range (-16 °C to 33 °C). Furthermore, the experimental data is suppressed at a high temperature range (> 33 °C). These results are inconsistent with the low resistivity interfacial region of the Maxwell–Wagner effect since this model always accompanies a high dielectric loss [23–26].

In Fig. 3 (a), the dielectric loss and dielectric constant of the PFWTM-1 ceramics are increased when the measured temperature is increased at low frequencies and higher temperature (> 50 °C). According to the previous reports [4,5], these phenomena are due to the space charge polarization and dc conduction which are presented in the previous section. In Fig. 4 (a), (b) and (c), these two-layer structure capacitors are compacted with the PFWTM-1 and PFWTM-2 ceramics. Therefore, the two-layer structure capacitors should exhibit the dielectric properties of the PFWTM-1 and PFWTM-2 ceramics. Furthermore, the 3:1 PFWTM should exhibit more the dielectric properties of the PFWTM-1 ceramics since the thickness of the PFWTM-1 ceramics is the largest. In Fig. 4, the dielectric loss is obviously increased when the measured temperature is increased at the highest temperature range (> 50 °C) for both the experimental data and the fitting results. For the fitting results shown in Fig. 4 (a), (b) and (c), the dielectric constant is obviously increased when the measured temperature is increased at the lower frequency and higher temperature (> 50 °C). For the experimental data of the 3:1 PFWTM shown in Fig. 4 (c), the dielectric constant is slightly increased when the measured temperature is increased at the low frequencies and higher temperature (> 80 °C). These phenomena show the dielectric properties of the PFWTM-1 ceramics at the high temperature and are enhanced by increasing the thickness of the PFWTM-1 ceramics at the same time. According to the dielectric properties of the PFWTM-1 ceramics and the response mechanism at the highest temperature (> 50 °C) in Fig. 3(a), it is concluded that the space charge polarization and the dc conduction also show at the highest temperature range ($>$ 50 °C) for the two-layer structure capacitors shown in Fig. 4 (a), (b) and (c). The experimental results are suppressed as compared the fitting results. Therefore, it is concluded that the space charge polarization and the dc conduction are suppressed at the highest temperature range by the two-layer structure since the phenomena of increased dielectric constant and loss with increased temperature at the highest temperature are suppressed.

4. Conclusions

In conclusion, this study investigated the low field dielectric responses of the two-layer structure capacitors with different compositions for the different thickness ratios of the PFWTM-1 and PFWTM-2 ceramics. The experimental data of the two-layer structure capacitors compare the Maxwell–Wagner effect fitted with the experimental data of the PFWTM-1 and PFWTM-2 ceramics with single-layer structure. With the two-layer structure, temperature-independent dielectric peaks are realized and the dielectric constant is enhanced. Moreover, the dielectric loss is obviously suppressed at the high temperature range for the experimental data of the two-layer structure capacitors. It is concluded that the space charge polarization and the dc conduction are reduced at the highest temperature region for the two-layer structure capacitors. The temperature-independent dielectric peak and the enhanced dielectric constant can be explained by the Maxwell–Wagner model with a low resistivity interfacial region. However, until now, other phenomena could not be adequately explained by a physical model. We will continue with further research and quantitative analysis in the future.

Acknowledgments

This research was supported by the National Science Council of Republic of China, under grant NSC-99-2221-E-017-005.

References

[1] L.E. Cross, Ferroelectrics 76 (1987) 241–267.
[2] L.E. Cross, Ferroelectrics 151 (1994) 305–320.
[3] T.R. Shrout, A. Halliyal, American Ceramic Society Bulletin 66 (1987) 704–711.
[4] D. Szwagierczak, J. Kulawik, Journal of the European Ceramic Society 25 (2005) 1657–1662.

[5] L. Zhou, P.M. Vilarinho, J.L. Baptista, Journal of Applied Physics 85 (1999) 2312–2317.
[6] L. Mitoseriu, P.M. Vilarinho, J.L. Baptista, Applied Physics Letters 80 (2002) 4422–4424.
[7] L. Mitoseriu, P.M. Vilarinho, M. Viviani, J.L. Baptista, Materials Letters 57 (2002) 609–614.
[8] L. Mitoseriu, M.M. Carnasciali, P. Piaggio, P. Nanni, Journal of Applied Physics 96 (2004) 4378–4385.
[9] L. Mitoseriu, A. Stancu, C. Fedor, P.M. Vilarinho, Journal of Applied Physics 94 (2003) 1918–1925.
[10] C.-S. Hong, S.-Y. Chu, W.-C. Su, R.-C. Chang, H.-H. Nien, Y.-D. Juang, Journal of Applied Physics 101 (2007) 054117.
[11] C.-S. Hong, S.-Y. Chu, C.-C. Tsai, C.-C. Hsu, Ceramics International 37 (2011) 1911–1918.
[12] G.-F. Chen, S.-L. Fu, IEEE Transactions on Components, Hybrids, and Manufacturing Technology 11 (1988) 600–603.
[13] Z. Zhu, N. Zheng, G. Li, Q. Yin, Journal of the American Ceramic Society 89 (2006) 717–719.
[14] Y. Hou, M. Zhu, F. Gao, H. Wang, B. Wang, H. Yan, C. Tian, Journal of the American Ceramic Society 87 (2004) 847–850.
[15] Z. Abdelkafi, N. Abdelmoula, O. Bidault, H. Khemakhem, M. Maglione, Physica B 406 (2011) 3470–3474.
[16] D.C. Sinclair, T.B. Adams, F.D. Morrison, A.R. West, Applied Physics Letters 80 (2002) 2153–2155.
[17] L. Ni, X.M. Chen, Applied Physics Letters 91 (2007) 122905.
[18] T.B. Adams, D.C. Sinclair, A.R. West, Advanced Materials 14 (2002) 1321–1323.
[19] P. Lunkenheimer, R. Fichtl, S.G. Ebbinghaus, A. Loidl, Physical Review B 70 (2004) 172102.
[20] C.C. Wang, Y.M. Cui, L.W. Zhang, Applied Physics Letters 90 (2007) 012904.
[21] M.H. Cohen, J.B. Neaton, L. He, D. Vanderbilt, Journal of Applied Physics 94 (2003) 3299–3306.
[22] C.C. Wang, L.W. Zhang, Applied Physics Letters 88 (2006) 042906.
[23] C.C. Wang, H.B. Lu, K.J. Jin, G.Z. Yang, Modern Physics Letters B 22 (2008) 1297–1305.
[24] G. Catalan, D. O'Neill, R.M. Bowman, J.M. Gregg, Applied Physics Letters 77 (2000) 3078–3080.
[25] D. O'Neill, R.M. Bowman, J.M. Gregg, Applied Physics Letters 77 (2000) 1520–1522.
[26] M. Xiao, Materials Letters 51 (2001) 135–138.
[27] Y.J. Li, X.M. Chen, R.Z. Hou, Y.H. Tang, Solid State Communications 137 (2006) 120–125.
[28] Y.Q. Lin, X.M. Chen, Materials Chemistry and Physics 117 (2009) 125–130.
[29] W. Eerenstein, N.D. Mathur, J.F. Scott, Nature 442 (2006) 759–765.
[30] D. Zhou, H. Wang, X. Yao, Materials Chemistry and Physics 105 (2007) 151–153.
[31] D. Zhou, L.X. Pang, H. Wang, J. Guo, X. Yao, C.A. Randall, Journal of Materials Chemistry 21 (2011) 18412–18420.
[32] C.-S. Hong, S.-Y. Chu, B.-J. Li, W.-C. Su, R.-C. Chang, H.-H. Nien, Y.-D. Juang, Journal of Applied Physics 103 (2008) 094102.